Intra-field On-Product Overlay improvement by application of RegC® and TWINSCAN™ corrections

Ofir Sharoni[a], Vladimir Dmitriev[a], Erez Graitzer[a], Yuval Perets[a], Kujan Gorhad[a]
Richard van Haren[b], Hakki Ergun Cekli[b], Jan Mulkens[b]
[a]Carl Zeiss SMS Ltd., 44 Maale Camon, Karmiel, 21613 Israel
[b]ASML, Flight Forum 1900 (no. 5846), 5657 EZ Eindhoven, The Netherlands;

ABSTRACT

The on product overlay specification and Advanced Process Control (APC) is getting extremely challenging particularly after the introduction of multi-patterning applications like Spacer Assisted Double Patterning (SADP) and multi-patterning techniques like N-repetitive Litho-Etch steps (LE^N, $N \geq 2$). When the latter is considered, most of the intra-field overlay contributors drop out of the overlay budget. This is a direct consequence of the fact that the scanner settings (like dose, illumination settings, etc.) as well as the subsequent processing steps can be made very similar for two consecutive Litho-Etch layers. The major overlay contributor that may require additional attention is the Image Placement Error (IPE). When the inter-layer overlay is considered, controlling the intra-field overlay contribution gets more complicated. In addition to the IPE contribution, the TWINSCAN™ lens fingerprint in combination with the exposure settings is going to play a role as well. Generally speaking, two subsequent functional layers have different exposure settings. This results in a (non-reticle) additional overlay contribution.

In this paper, we have studied the wafer overlay correction capability by RegC® in addition to the TWINSCAN™ intra-field corrections to improve the on product overlay performance. RegC® is a reticle intra-volume laser writing technique that causes a predictable deformation element (RegC® deformation element) inside the quartz (Qz) material of a reticle. This technique enables to post-process an existing reticle to correct for instance for IPE. Alternatively, a pre-determined intra-field fingerprint can be added to the reticle such that it results in a straight field after exposure. This second application might be very powerful to correct for instance for (cold) lens fingerprints that cannot be corrected by the scanner itself. Another possible application is the intra-field processing fingerprint. One should realize that a RegC® treatment of a reticle generally results in global distortion of the reticle. This is not a problem as long as these global distortions can be corrected by the TWINSCAN™ system (currently up to the third order). It is anticipated that the combination of the RegC® and the TWINSCAN™ corrections act as complementary solutions. These solutions perfectly fit into the ASML Litho InSight (LIS) product in which feedforward and feedback corrections based on YieldStar overlay measurements are used to improve the on product overlay.

Keywords: Registration Error, Overlay, Reticle, Mask, LELE, RegC®, LIS, Fingerprint Correction

1. INTRODUCTION

One of the key factors to high yield in a wafer fab production environment is the on-product overlay performance. As the technology shrinks, one functional layer could no longer be exposed as a single layer by one single mask. Over time, more and more mask exposures followed by hard mask etch steps are required to create a single functional layer for a given device. The mask contribution as part of the total on-product overlay budget in a multi-patterning layer cannot be neglected anymore [1]. Within one functional layer, the mask-to-mask overlay errors can be reduced by writing the masks on the same e-beam writer one after the other. However, in case multiple mask sets for different functional layers need to be optimized with respect to each other, this may not be so trivial anymore. Higher order intra-field process corrections are required to bring the on-product overlay to the required performance levels.

*Ofir.Sharoni@zeiss.com; phone +972 4 9088 620; Mobile +972-526477801; fax +972 4 9088 666; www.zeiss.com/sms
*Richard.van.Haren@asml.com; Mobile : +31-6-11786083; fax +31-402685430; www.asml.com

The origin of the higher order intra-field overlay contribution can come from several sources. One obvious one comes from the e-beam mask writer itself. It may leave a tool specific writing fingerprint behind. Moreover, it may drift over time. Masks that are produced on different generations of writing tools may have different fingerprints as well. Another source is the scanner itself. Each functional layer is exposed using a unique, optimized, illumination setting. In case the functional layer is composed out of several sub-layers, the illumination conditions for these sub-layers are likely to be very similar. However, when two different functional layers are considered (e.g. the gate and contact layer) the illumination settings are not the same and a residual intra-field lens fingerprint may remain. The reason is that different parts of the lens are used resulting in an intra-field fingerprint. A third source that leads to higher order intra-field overlay penalties that needs to be mentioned here is an intra-field processing contribution. These contributions may arise from pattern density differences within the die and their impact on the etching performance (e.g. misplacement). In addition, local distortion may show up when etching stressed layers. In general, these effects can be effectively suppressed by intra-field higher order process corrections (*i*HOPC) [2]. However, whatever model is applied, residuals remain. The main goal of this paper is to explore the on-product overlay correction capability to beyond what is currently possible. As a first step, the correction capabilities of RegC® [3] are investigated.

Based on the above, there are basically 3 different approaches, using the reticle (intra-field effect), for reduction the magnitude of wafer overlay residuals:

- Controlling the mask to mask overlay in the mask shop. Especially for multi-patterning applications this would be of great value.
- Controlling the mask registration specification in the mask shop. This application is aiming to reduce the high order residuals that might still be present after mask production.
- Controlling the wafer overlay directly in the wafer FAB. In this use case, the measured on-product overlay contains contributions from the scanner, mask, and process.

The main goal of this paper is to explore the correction capabilities of the RegC® in reducing the mask registration fingerprint or alternatively inducing a pre-defined one. We take a holistic view and consider the corrections within a larger framework, see Fig. 1. On top of the figure we see the lithography cluster consisting of the ASML TWINSCAN™ and the track that may include a Yield Star Inline Metrology tool. The scanner settings (actuators) can be adjusted via an external interface (overlay optimizer) by means of control software (Litho InSight or LIS). In principle, the control software can be fed by different sources of input data. Either on-product overlay measurements from metrology tools (inline or offline) or even external data sources. Before feeding the corrections to the scanner, a balanced optimization can be made by taking the limits of the actuator ranges into account.

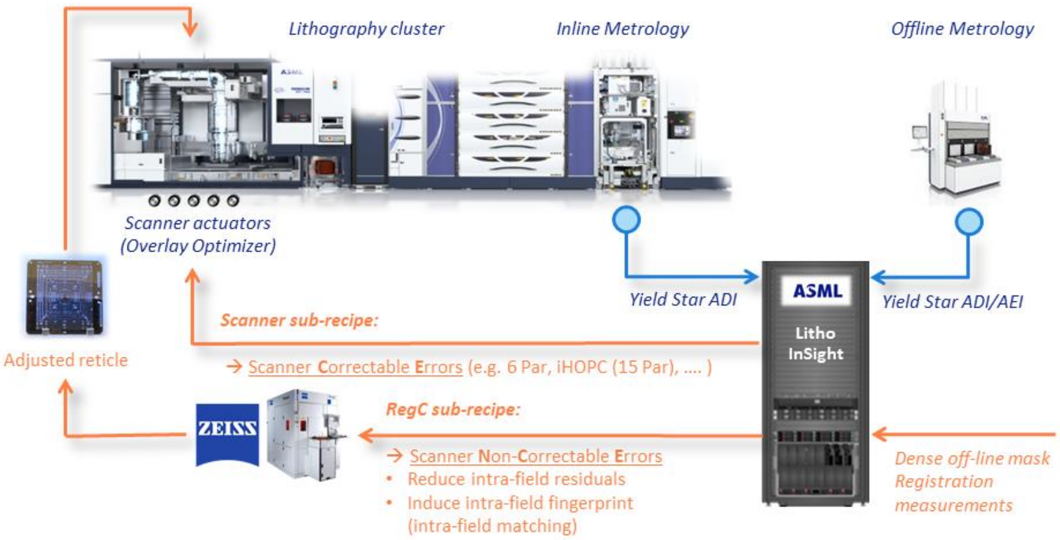

Figure 1. Frame work in which the current work is positioned. Only the part marked in orange is addressed in this paper. It shows the co-optimization of the TWINSCAN™ and RegC® corrections within the Litho InSight (LIS) concept.

Let's now consider the orange marked text and arrows in figure 1. The first branch labelled with "scanner sub-recipe" was already addressed in an earlier publication [1]. In that work, the possibility of feeding corrections based on offline mask registration measurements to the scanner was explored. The prime focus was first on the linear terms (translation, magnification, and rotation). It was demonstrated that the measured residuals on wafer were in perfect agreement with the mask registration residuals. This observation implies that the concept of sending feed-forward corrections to the scanner also works for the non-linear terms. We will report on this more extensively later in time. Basically, all (future) scanner correctable terms can be addressed via this branch.

The second branch labelled with "RegC® sub-recipe" is complementary to the first one. It addresses the scanner non-correctable errors. While the scanner can currently only correct for the global (up to the third order polynomial) intra-field overlay errors, the RegC® corrections can address the remaining part. It is anticipated that this part of the overlay budget can still be quite significant and will become more relevant in the future due to the tighter overlay specifications. In addition to on-product wafer overlay measurements, input data from offline mask registration measurements give valuable information on how to optimize the masks and/or mask sets. The requirements on the quality of the offline registration measurements are high: the input data to the RegC® must be both accurate and repeatable. In this work the ZEISS PROVE® tool was used for this purpose [4]. We would like to note that the ZEISS PROVE®-RegC® closed loop is an already proven solution for measuring and correcting the mask registration and the mask-to-mask overlay (OVL) errors in the mask shop [5].

In the remainder of this paper, the focus will be on the RegC® tool capability to reduce or induce (pre-define) mask fingerprints. One should keep in mind that this work is performed within a larger framework (Litho InSight) aiming to improve the on-product overlay performance.

2. EXPERIMENTAL DETAILS

2.1 Experimental goal

In order to improve the intra-field on-product overlay requirements, the goal of the current work is two-fold:

- Explore the correction capability of RegC® to <u>reduce</u> the mask registration fingerprint.
- Explore the correction capability of RegC® to <u>induce</u> a pre-defined mask registration fingerprint.

The reduction of the mask registration fingerprint is a logical step in achieving a better on-product overlay performance. The mask writing error directly contributes to the measured overlay on wafer. Since the mask contribution has become a dominant part in the multi-patterning on-product overlay budget, all techniques that help to reduce this part of the budget are highly encouraged. Moreover, it helps to simplify the overlay control strategies.

The second goal seems to be less obvious at first sight. The mask registration gets worse after adding a pre-defined fingerprint. However, when two (or multiple) masks are considered, the on-product overlay performance can be significantly improved. Since there is a tendency to optimize multiple layers for overlay at the same time to create yielding devices, this correction capability may become very powerful.

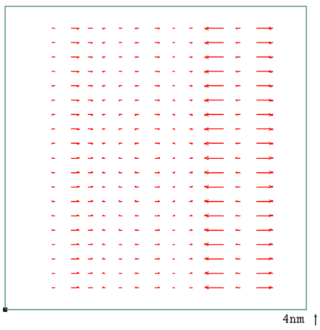

Figure 2. Pre-defined imposed intra-field fingerprint. The challenging part is on the right-hand side of the mask (3 last columns). The registration errors ~8-nm in magnitude (4×, Mask level) change direction over relatively short distance.

In figure 2 we show an example of the challenging intra-field fingerprint we have selected to add to one of the masks under investigation. The fingerprint is imposed on a 13 × 19 layout at mask level (4×) and it contains an interesting signature on the right-hand side. The 13 × 19 layout has a pitch of 8480-µm and 7208-µm in *x* and *y*, respectively. The registration errors we impose are in the order of ~8-nm in magnitude (~2-nm at wafer level) and pointing in opposite directions. The signature is challenging since it cannot easily be corrected by a third order polynomial.

2.2 Work flow

In order to reach the experimental goals mentioned in section 2.1, the schematic work flow shown in figure 3 was followed.

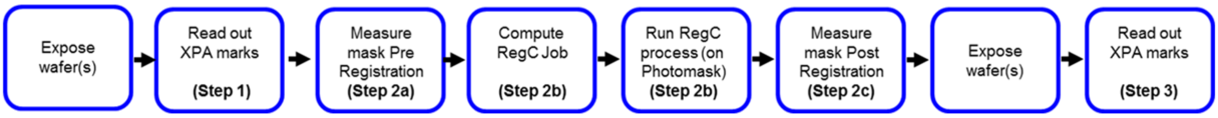

Figure 3. Work flow to reduce and induce mask registration fingerprints. The ASML TWINSCAN™ is used for step 1 and step3. The ZEISS RegC® tool is used to correct the mask finger prints (Step 2b) and the ZEISS PROVE® tool to provide the offline mask registration measurements (Step 2a and 2c).

Below we address the important steps in the work flow and some key aspects are highlighted.

- Step 1. All the exposures and scanner readouts were done on ASML TWINSCAN™ systems. Three state-of-the art set-up and qualification masks (A, B, and C) have been used together with 12 (3×4) etched reference wafers. Four wafers are used per mask. This enables us to average out wafer-to-wafer effects and [since many fields (68) are averaged] to focus on the average field only. The masks contain so-called XPA alignment marks in a 13×19 layout that can be read out by the scanner. This can be done with respect to the etched reference layer having the same 13×19 layout or to the nominal grid. Each wafer can also be used to accommodate multiple layer exposures. In that case a different shift is applied per exposed layer. Three masks are considered:
    - Mask A: This mask is dedicated for reducing the mask registration fingerprint by the RegC® process.
    - Mask B: This mask is intended to reduce the initial mask registration fingerprint and to add a pre-defined intra-field fingerprint by the RegC® process.
    - Mask C: This mask will not be treated by the RegC® process. It is used to monitor and correct for the scanner changes before (PRE) and after (POST) the RegC® treatment of Masks A and B.

  The TWINSCAN™ readouts are referred to as $\text{SCANNER}_{\text{PRE-Mask-A}}$ and $\text{SCANNER}_{\text{PRE-Mask-B}}$.
- Step2a. Before the RegC® process is performed on Masks A and B, registration measurements are done using the PROVE® registration measurement tool. These pre-RegC® measurements are labeled $\text{PROVE}^{®}_{\text{PRE-Mask-A}}$ and $\text{PROVE}^{®}_{\text{PRE-Mask-B}}$, respectively.
- Step2b. This step refers to the actual RegC® treatments of Masks A and B. The input for the RegC® job is based on $\text{PROVE}^{®}_{\text{PRE-Mask-A}}$ measurements for Mask A. For Mask B, the $\text{PROVE}^{®}_{\text{PRE-Mask-B}}$ data with the addition of the pre-defined intra-field fingerprint as shown in Figure 2 is used as input.
- Step 2c. This step refers to the PROVE® registration measurements after the RegC® process on Mask A and B were carried out. These measurements are labelled as $\text{PROVE}^{®}_{\text{POST-Mask-A}}$ and $\text{PROVE}^{®}_{\text{POST-Mask-B}}$.
- Step 3. This is the final step in the work flow. Exposures are performed with RegC® treated Masks A and B and the monitoring Mask C. TWINSCAN™ readouts are performed and the data obtained is referred to as $\text{SCANNER}_{\text{POST-Mask-A}}$ and $\text{SCANNER}_{\text{POST-Mask-B}}$.

All the TWINSCAN™ measurements presented in this paper have been corrected for the scanner status change in between step 1 and step 3 ($\Delta\text{SCANNER}_{\text{Mask-C}} = \text{SCANNER}_{\text{POST-Mask-C}} - \text{SCANNER}_{\text{PRE-Mask-C}}$).

2.3 RegC® concept explanation

In this section, we would like to elaborate more on the RegC® process (step 2b in the previous section). The now well-established RegC® process [3] uses a femto-second pulse laser to write pixels (deformation elements) inside the mask fused silica bulk that affect the image placement at the mask absorber level in order to compensate for the registration and or overlay problems.

The deformation can be described by a physical-mathematical model of a two-dimensional rectangular cell. The basic deformations can be described by pixels having different shapes and orientations. These so-called Mode Signatures (MS) are illustrated in Figure 4 and labelled a, b, c and d.

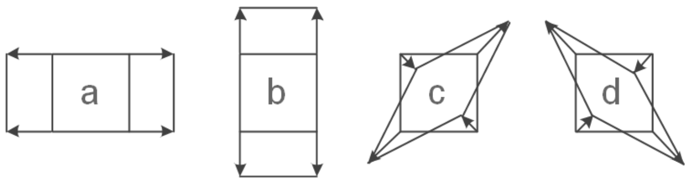

Figure 4. Illustration of the Mode Signatures (MS). Four different modes exists, horizontal and vertical mode (*a* and *b*) as well as two diagonal Modes (*c* and *d*).

The model describes a cumulative effect of multitude pixels in the quartz substrate when taking into account the physical properties of fused silica. The mode signature (MS) is defined as the angle and deformation magnitude induced by the pixels at a certain condition. Typically the RegC® process utilizes two different modes with different deformation properties. Each mode has its own signature that is described by three basic parameters in figure 4. The MS parameters are derived utilizing an in situ metrology system that can measure and quantify the pixels deformation properties.

A typical RegC® job is a combination of these two modes. In the current work, the use of the two diagonal modes (*c* and *d* in Fig. 4) is presented. The reason to select the two diagonal modes is that these modes are better suited to correct for the intra-field fingerprint obtained from the PROVE® tool measurements. One can imagine that using all four modes enables a more accurate correction of the registration and/or overlay problem. Basically, two more degrees of freedom of correction are added resulting in a better efficiency of the RegC® process.

The RegC® pixels induce an expansion of the quartz bulk. This means that the absolute registration value (raw data) after the RegC® process will be larger than before the process. This is not an issue as long as this induced signature can be corrected by the scanner. The main part of these corrections can be described by a linear (6 parameter) model in terms of Translation, Magnification, and Rotation (*Tx, Ty, Mx, My, Rx, Ry)*. These corrections can easily be made during reticle alignment on the scanner.

The RegC® process can also be optimized in a way that it transfers the scanner non-correctable registration errors into a systematic fingerprint that can be corrected by the TWINSCAN™. Within the Litho InSight framework, the scanner correctable fingerprints are not restricted to linear corrections only. The full scanner correction capability can be utilized. Therefore, in some use cases it might be beneficial to optimize the RegC® job in order to transform non-correctable errors into a higher order intra-field fingerprint. The co-optimization of both the RegC® and TWINSCAN™ corrections within the Litho InSight framework enables to control the on-product overlay performance better than the individual corrections alone.

3. RESULTS

3.1 Pre-RegC® reticle registration data

After exposure and read-out the wafers on the TWINSCAN™, Mask A and B were shipped to perform the registration measurements on the PROVE® tool. The measurements are corrected by a 6 parameter (linear) model and the results for both masks at mask level (at 4×) are shown in figure 5. It is obvious that the registration fingerprint on both masks look

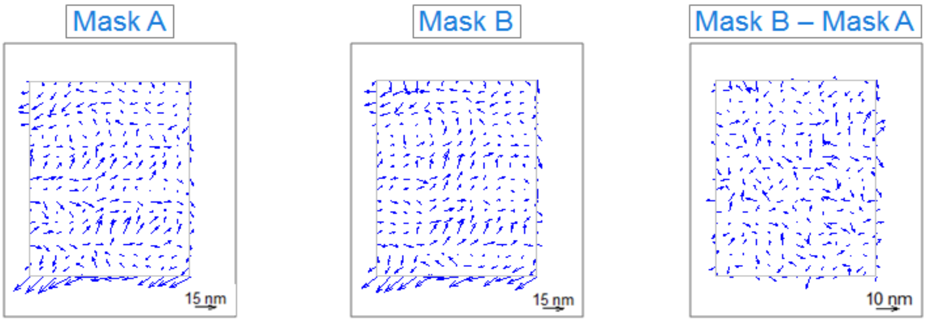

Figure 5. Mask registration measurements (4×). These measurements were performed before the RegC® process was performed and were referred to as PROVE®$_{\text{PRE-Mask-A}}$ and PROVE®$_{\text{PRE-Mask-B}}$, respectively.

very similar. This is expected due to the fact that the masks are written on the same mask writing tool one after the other. The 3σ values of the registration errors are around 12-nm for both masks (PROVE®$_{\text{PRE-Mask-A}}$ and PROVE®$_{\text{PRE-Mask-B}}$). When considering the difference between the two masks, the 3σ value of the distribution is around 6-nm. This corresponds to 1.5-nm at wafer level (1×). Note that this observation is in line with the earlier considerations regarding the multi-patterning use case. Although the mask-to-mask registration delta might still be ok, this is not necessarily the case for the individual mask to its nominal grid or to a mask used in the previous layer. In case the mask is specified according a 3σ value irrespective of the fingerprint, one can expect a penalty of $\sqrt{2}\cdot(3\sigma)$. This is very likely to happen when masks of successive layer are manufactured on different e-beam mask writing tools or when the tools drift over time.

3.2 RegC® simulations and process

After the PROVE®$_{\text{PRE-Mask-A}}$ and PROVE®$_{\text{PRE-Mask-B}}$ registration measurements were obtained, the masks were shipped to a different location in order to apply the RegC® process. The RegC® process calculations were based on the RegC® Wizard software shown in figure 6.

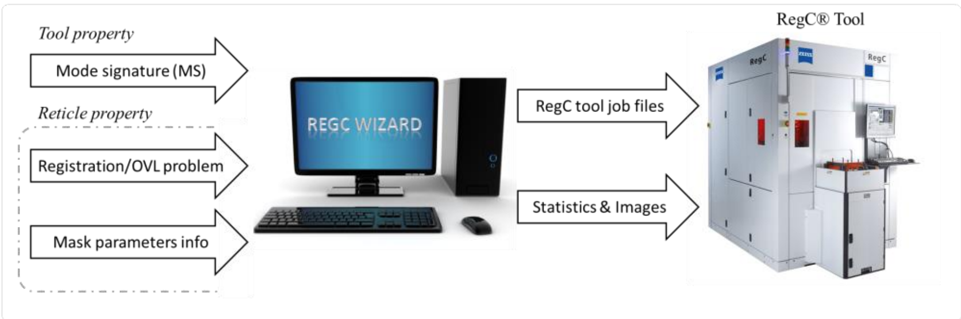

Figure 6. Inputs/outputs of the supporting software: the RegC® Wizard. The mode signature is an important input parameter to optimize the mask fingerprint.

The Mode Signatures (MS) used for Mask A & Mask B were the two diagonal MS presented in Figure 4 (c and d). Since the MS represented the pixels orientation, each MS will have a different influence on the mask pattern deformation. All four MS combinations can influence any registration vector orientation. Given the PROVE®$_{\text{PRE-Mask-A}}$ and PROVE®$_{\text{PRE-Mask-B}}$ mask fingerprints, it was decided to choose the two diagonals MS out of the four possibilities. The choice was made based on the fact that this was the most efficient way to reduce this type of fingerprint by these two modes.

The RegC® Wizard computes the desired pixels locations and density for each Mode. Since two Mode Signatures are chosen, the RegC® wizard supplies two files (Job Files), one for each Mode. The job files are part of one recipe that runs automatically on the RegC® tool. Additionally, the RegC® Wizard also supplies images of the pixel location and density.

This is illustrated in figure 7 for Mask A. The pixels locations & density have an impact on the exposure dose. The combination of the two jobs ensures uniform attenuation across the mask active area and hence neutral effect on CDU.

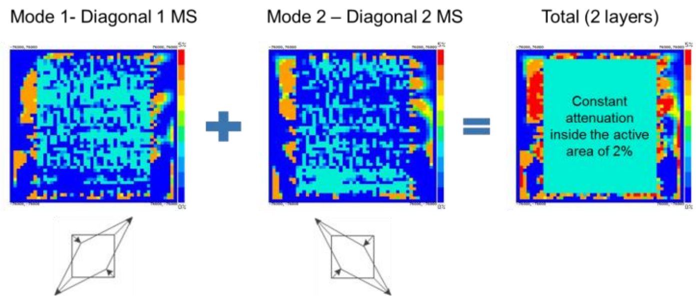

Figure 7. Two jobs (one for each mode) used to optimize Mask A registration fingerprint. The location and density of the pixels is chosen in a way that the CDU is not impacted. A constant attenuation (2%) inside the active area remains.

Figure 8 shows the expected results after the RegC® treatment of Mask A. The input data for the RegC® Wizard is based on PROVE®$_{\text{PRE-Mask-A}}$ input data set. It is evident that the quality of the input data is extremely important to enable the proper corrections of the mask. The reduction in residuals is huge, ~80% in *x* and ~55% in *y*.

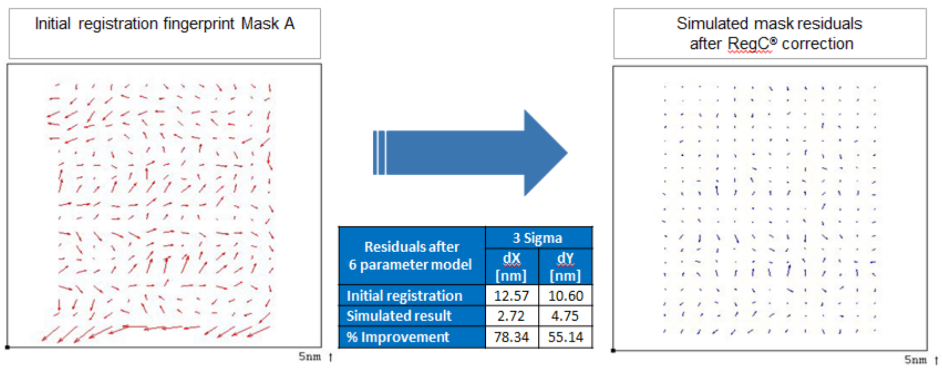

Residuals after 6 parameter model	3 Sigma dX [nm]	3 Sigma dY [nm]
Initial registration	12.57	10.60
Simulated result	2.72	4.75
% Improvement	78.34	55.14

Figure 8. Mask A registration measurements (at 4×, Mask level). A large reduction of the residuals is expected after the RegC® process.

This implies that the mask residuals on wafer are expected to drop from (3.1, 2.6) to (0.7, 1.2) nanometer. The RegC® treatment for Mask B (Fig. 9) is more challenging. The goal for this mask is reducing/eliminating the initial registration fingerprint (PROVE$_{\text{PRE-Mask-A}}$) and to add a pre-defined intra-field fingerprint as presented in figure 2.

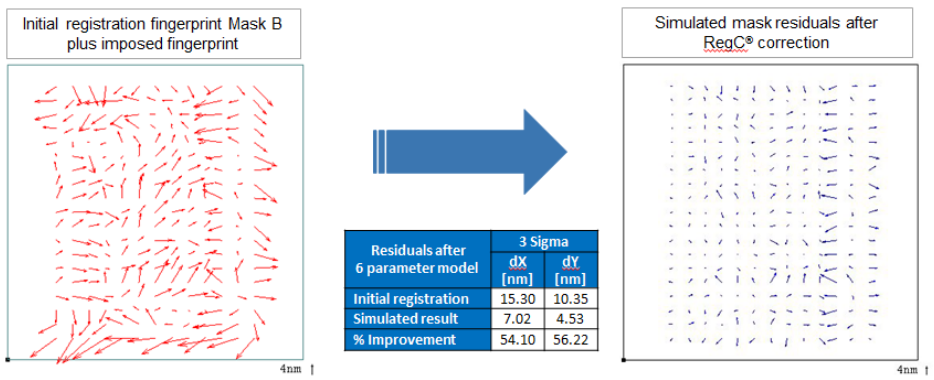

Residuals after 6 parameter model	3 Sigma dX [nm]	3 Sigma dY [nm]
Initial registration	15.30	10.35
Simulated result	7.02	4.53
% Improvement	54.10	56.22

Figure 9. Mask B registration measurements plus the pre-defined intra-field fingerprint (at 4×, Mask level). Overall, the registration residuals are strongly reduced after the RegC® process.

The resulting “mask” is artificial in a way, since the added intra-field fingerprint is not really present on the physical mask itself. However, this data set can be used as input data for the RegC® treatment. Also in this case, the expected reduction in registration residuals is significant (~50%). Surprisingly, the imposed intra-field signature seems to still be present in the expected residuals after RegC® treatment. However, a closer look reveals that the imposed intra-field signature is suppressed to some extent. We decided to quantify this effect first. This was done by continuing the work flow with this input data and to look at the $\text{PROVE}^{®}_{\text{POST-Mask-B}}$ and $\text{SCANNER}_{\text{POST-Mask-B}}$.

It should be noted that if we feed the RegC® Wizard with the challenging intra-field signature (←→), the opposite signature is expected on the real mask (→←). This is due to the fact that the imposed intra-field fingerprint is artificial.

3.3 Post-RegC® reticle registration data and wafer results

Let’s first consider Mask A results. Figure 10 shows the PROVE® measurement results before and after the RegC® process was applied to Mask A. The $\text{PROVE}^{®}_{\text{POST-Mask-A}}$ mask residuals indeed drop down to the required ~1.5-nm at wafer level (1×). This level can be compared to the mask-to-mask difference as discussed in the introduction section. The similarity between the $\text{PROVE}^{®}_{\text{POST-Mask-A}}$ fingerprint and the simulated residuals by the RegC® Wizard is striking. This strongly indicates that input data for the RegC® mask treatment is directly found back on the mask after treatment.

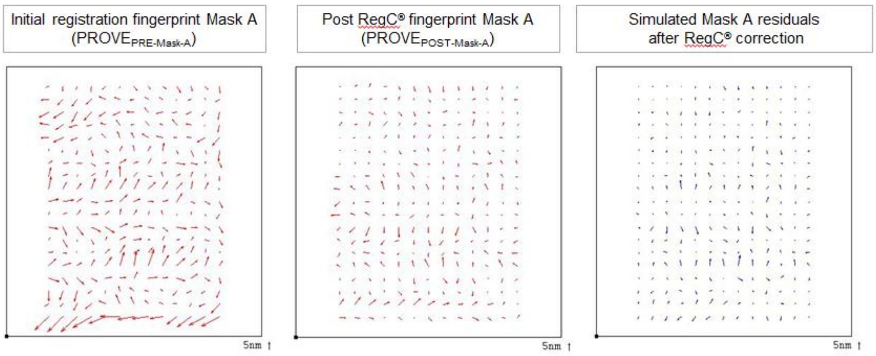

Figure 10. Mask A registration measurements PRE and POST the RegC® process as measured by the PROVE® tool (4×). The POST RegC® fingerprint can be directly compared with the simulated residuals by the RegC® Wizard.

Since we have used an ASML setup and qualification mask we investigated the mask’s fingerprint change measured by TWINSCAN™ before and after the RegC® treatment as well. It can be directly compared with the PROVE® tool measurements. The mask change as measured by the PROVE® tool is equal to $\Delta\text{PROVE}^{®}_{\text{Mask-A}} = \text{PROVE}^{®}_{\text{POST-Mask-A}} - \text{PROVE}^{®}_{\text{PRE-Mask-A}}$. This delta fingerprint can be compared with the RegC® expected simulation results. The results (now at wafer level, 1×) are shown in figure 11. In addition, we also verified this change in fingerprint with SCANNER on-wafer measurements.

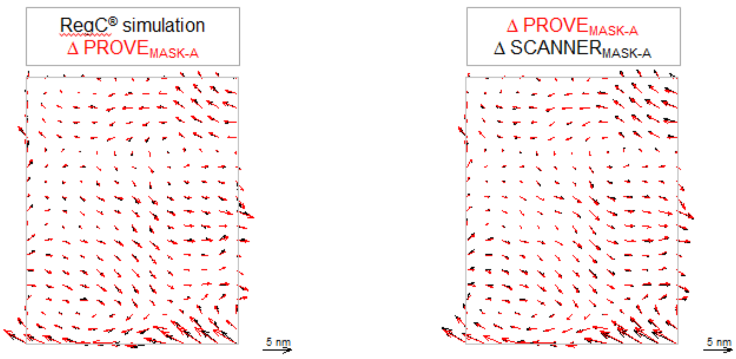

Figure 11. A direct comparison between the RegC® simulation results and the ΔPROVE® measurements (Post minus Pre) is shown. The PROVE® measurements can also be compared with the SCANNER results (right-hand side picture). Perfect correlations are observed.

The scanner intra-field difference ($\Delta SCANNER_{Mask\text{-}A}$) cannot be used directly, it needs to be corrected with status change of the scanner ($\Delta SCANNER_{Mask\text{-}C}$). The implementation of the monitoring reticle in the test plan now turns out to be of crucial importance. In fact, the post-RegC® exposures and read out was done on a different scanner (NXT: 1970i) while the NXT: 1960i was used before the RegC® treatment of both masks. After taking this correction into account, the $\Delta SCANNER_{Mask\text{-}A}$ can be directly compared with the $\Delta PROVE_{Mask\text{-}A}$ measurements. The results are also shown in figure 11. Perfect correlation between the PROVE® measurements and the SCANNER measurements is observed.

For Mask B, the story is similar to the above. Also in this case the observations are in line with those of Mask A. The initial mask fingerprint ($PROVE_{PRE\text{-}Mask\text{-}B}$) was effectively suppressed. The intention for Mask B was different though: in this case the interest was mainly on the pre-defined imposed intra-field fingerprint. Although the expectations were not very high as already was outlined in section 3.2, we still tried to find back the expected corrections on the mask.

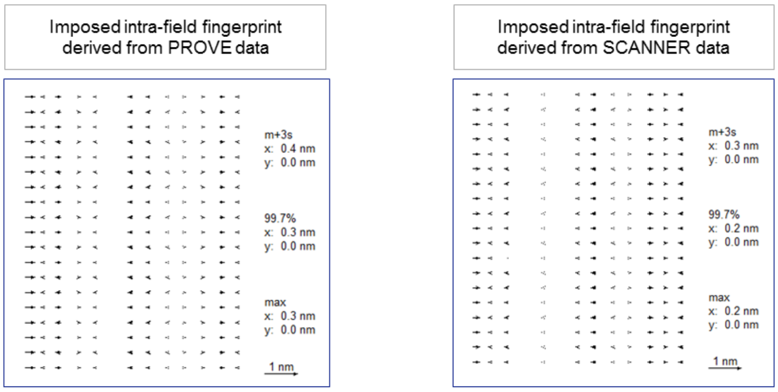

Figure 12. Imposed intra-field fingerprint (column average) derived from PROVE® and SCANNER (on-wafer) measurements. The magnitude of the signature is small ~0.3-nm but still observable (→←) on the left-side of the field.

We indeed succeeded in finding the imposed intra-field signature back in the measured data. It should be noted however that this was only possible after looking at the column average. Similar results have been obtained both from the PROVE® measurements as well as from the SCANNER measurements. Although small, around 0.2-nm to 0.3-nm the signature we were looking for (→←) could indeed be isolated. This particular signature (→←) was found in column 1 and 3 on the left-hand side of the field. The location inside the field is now on the left-hand side. This is due to the fact that the mask is loaded chrome side down on the scanner. We also see that the signature has flipped direction from (←→) to (→←). This is also expected and a consequence of the input signature for RegC®.

4. DISCUSSION

We realize that the focus of this paper is mainly on registration/overlay errors that cannot be corrected by the scanner actuators (the so-called scanner non-correctable errors). Since RegC® can be targeted to reduce these scanner non-correctable errors; it perfectly fits in the ASML Litho InSight (LIS) concept. Co-optimization of both correctable and non-correctable errors within this concept makes it so powerful. A balanced decision can be made between the corrections that can be fed directly to the scanner and the ones that can be used to optimize the mask via the RegC® tool. It is anticipated that more and more tailored functionalities will be added over time. It is very likely that the separation between scanner correctable errors and non-correctable errors change over time. Current non-correctable errors may later change into scanner correctable errors when more actuators become available via the Overlay Optimizer products.

Although the results presented in this paper are very promising, we still are exploring further opportunities to improve the on-product overlay. One new extension that is already on the roadmap is the utilization of 4 Mode Signatures for the RegC® process. The predicted simulation results are presented in figure 14. The shown field fingerprints are all shown at mask level (4×) and the input intra-field signature is quite large. The magnitude is +/- 8-nm is on the high side but it enables to study the capability of the corrections. It is clear that the signature can be suppressed significantly to levels below 1-nm on wafer when 4 Mode Signatures are used.

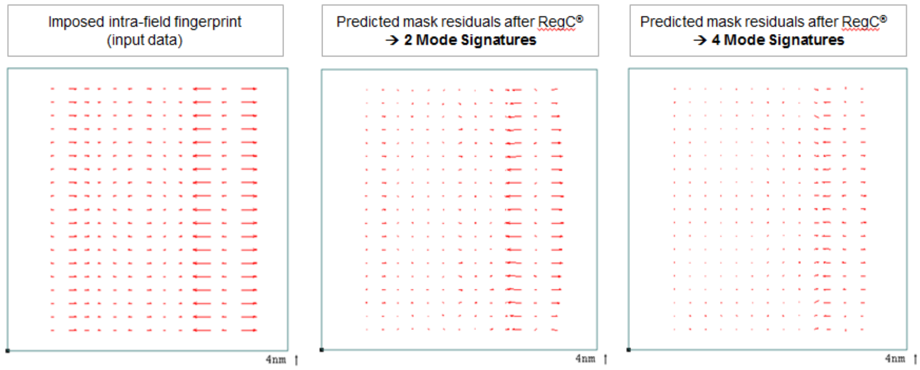

Figure 14. The RegC® correction capability can be extended to 4 Mode Signatures in the future. Currently, the mask corrections are based on 2 Mode Signatures.

5. CONCLUSIONS

In conclusion, we have presented a new concept in which the RegC® product is embedded in the ASML Litho InSight frame work. This offers the opportunity to enable a balanced optimization of the corrections. The correctable errors can be directly sent to the scanner as sub-recipe while the remaining non-correctable errors can be provided to the RegC® tool to optimize the mask fingerprint. Based on the required on-product overlay specification, it can be of large value to add a pre-defined fingerprint to one (or more) mask(s).

For this reason, two use cases have been explored. The first one was aimed to reduce the mask writing residual errors. More than a 50% improvement on the residual level was found. The improvements have been demonstrated by PROVE® and verified by TWINSCAN™ measurements.

The second use case shows similar improvement levels when considering the suppression of the overall mask residuals. Also in this case a reduction of more than 50% on residual level was found. The intention of the second use case was to add a pre-defined (challenging) intra-field fingerprint to one of the masks as well. Initially, 15% of this fingerprint was added to the mask. After reconsideration of the measured results, we realized that the corrections can be further improved by utilizing more correction capabilities of the RegC® tool.

Overall, the results presented in this paper look very promising and we are confident we can continue to extend the feasibility in a real wafer FAB.

ACKNOWLEDGEMENTS

ZEISS & ASML would like to have a special thank-you to Wolfgang Degel, Lucas Gui and Arthur Lee for their dedication performing the PROVE® measurements. The authors especially thank Budiman Sutedja for all his help he offered during the scanner exposures and measurements.

REFERENCES

[1] Richard van Haren, Hakki Ergun Cekli, Xing Lan Liu, Jan Beltman, Anne Pastol, Jean Massin, Emilie Dupre La Tour, Maxime Gatefait, Frank Sundermann, "Impact of reticle writing errors on the on-product overlay performance", Proc. of SPIE Vol. 9235 923522-1 (2014).

[2] Mulkens J, Hinnen P, Kubis M, Padiy A, Benschop J; "Holistic optimization architecture enabling sub-14-nm projection lithography". J. Micro/Nanolith. MEMS MOEMS. Volume 13, Issue 1, (2014).

[3] Kujan Gorhad, Avi Cohen, Dan Avizemer, Vladimir Dmitriev, Dirk Beyer, Wolfgang Degel, Markus Kirsch, "Further beyond – Registration & Overlay Control Enhancements for Optical masks," Proc. of SPIE Vol. 9235 92351P-8 (2014).

[4] D. Seidel, M. Arnz, D. Beyer; "In-die photomask registration and overlay metrology with PROVE® using 2D correlation methods", Proc. of SPIE Vol. 8166, 81661E (2011).

[5] Erez Graitzer, Avi Cohen, Vladimir Dmitriev, Itamar Balla, Dan Avizemer, Dirk Beyer, Klaus Boehm, Wolfgang Degel, "Closed Loop Registration Control (RegC®) Using PROVE® as the Data Source for the RegC® Process", Proc. of SPIE Vol. 8441 84410A-9 (2012).

[6] P. Leray, S. Cheng, A. Cohen, E. Graitzer, V. Dmitriev, S. Rehtan, N. Wertsman, "Compensating process non-uniformity to improve wafer overlay by RegC®", Proc. of SPIE Vol. 9050 9050-39 (2014).

[7] B. Lee, I. Lee, Y. Hyun, S. Kim, C.-M. Lim, M. Kim, S. Park, "EUV overlay strategy for improving MMO", Proc. of SPIE Vol. 9048 9048-26 (2014).